Eur. Phys. J. A **14**, 53–61 (2002)
DOI 10.1140/epja/iepja1269

THE EUROPEAN PHYSICAL JOURNAL A

Light-charged-particle evaporation from hot ^{31}P nucleus at $E^* \sim 60$ MeV

D. Bandyopadhyay[1], C. Bhattacharya[1], K. Krishan[1], S. Bhattacharya[1,a], S.K. Basu[1], A. Chatterjee[2], S. Kailas[2], A. Shrivastava[2], and K. Mahata[2]

[1] Variable Energy Cyclotron Centre, 1/AF, Bidhan Nagar, Kolkata - 700 064, India
[2] Nuclear Physics Division, Bhabha Atomic Research Centre, Mumbai - 400 085, India

Received: 1 August 2001
Communicated by R.A. Ricci

Abstract. The inclusive energy spectra of light charged particles, such as, α, p, d and t, evaporated from the hot ^{31}P nucleus at an excitation energy $E^* \sim 60$ MeV, have been measured at various angles. The compound nucleus ^{31}P has been populated using two different entrance channel configurations; *i.e.*, ^{7}Li (47 MeV) + ^{24}Mg and ^{19}F (96 MeV) + ^{12}C reactions, leading to the same excitation energy of the compound system. It has been observed that the spectra obtained in the ^{7}Li (47 MeV) + ^{24}Mg reaction follow the standard statistical-model prediction with a spherical configuration of the compound nucleus. But, the spectra obtained in the ^{19}F (96 MeV) + ^{12}C reaction deviate from similar predictions of the statistical model both on higher- as well as on lower-energy sides. Considerable deformation was required to be incorporated in the calculation in order to reproduce the measured-energy spectra in this case. Dynamical trajectory model calculations were not found to play any significant role in explaining the differences in behaviour between the two cases under study. The observed discrepancy has been attributed to the difference in the angular-momentum distributions of the compound nuclei formed in the two reactions.

PACS. 24.60.Dr Statistical compound-nucleus reactions – 25.70.Gh Compound nucleus – 25.70.Jj Fusion and fusion-fission reactions

1 Introduction

In recent years, there has been a lot of interest to study the statistical properties of hot rotating nuclei produced through heavy-ion fusion reactions. High excitation energy favours the nucleus to de-excite through statistical emission of several light particles followed by γ decay. The de-excitation process is governed by the available phase spaces, *i.e.*, the nuclear level densities of both the parent and daughter nuclei, as a function of excitation energy, angular momentum and deformation. The evaporated light-charged-particle spectra in conjunction with the statistical-model calculations can be used to extract the statistical properties of the hot, rotating nuclei.

However, recent studies reveal that, at high excitation energy and angular momentum, the energy spectra of evaporated light charged particles, are no longer consistent with the standard statistical-model predictions. A large number of experiments have been performed in the last few years to study this anomaly over a wide range of compound nuclear masses ($A_{\rm CN}$) in the range $\sim$ 60–170, for example [1–12], and in most cases (with the exception of [1]), it has been found that the statistical model fails to explain the observed light-charged-particle energy spectra. Choudhury *et al.* [2] have measured the α-particle energy spectra in the reaction 214 MeV ^{32}S on ^{27}Al and observed that the measured spectra deviate considerably from the standard statistical-model predictions. La Rana *et al.* [3] have measured α-particle spectra in the reaction 190 MeV ^{40}Ar on ^{27}Al and have seen a similar discrepancy. The authors argued that in the statistical-model calculation, the emission barrier is considered as the fusion barrier of the two partners in the exit channel assuming their spherical configuration. It may be a good approximation at low excitation energy and angular momentum. But, when the nucleus is at high excitation energy and rotating with high spin, it is likely to be deformed in shape. Hence, the emission barrier will be lower if one considers that the α-particles are emitted preferentially along the larger axis. On the contrary, it has been claimed [4, 5] that, only deformation, unless it is unrealistically large, cannot affect the α-particle emission barrier much; however, the anomaly may be well explained by incorporating spin-dependent level density in the standard statistical-model prescription to modify the yrast line keeping the emission barrier unchanged. Recently, Charity *et al.* [7] have measured light-charged-particle spectra emitted in

[a] e-mail: saila@veccal.ernet.in

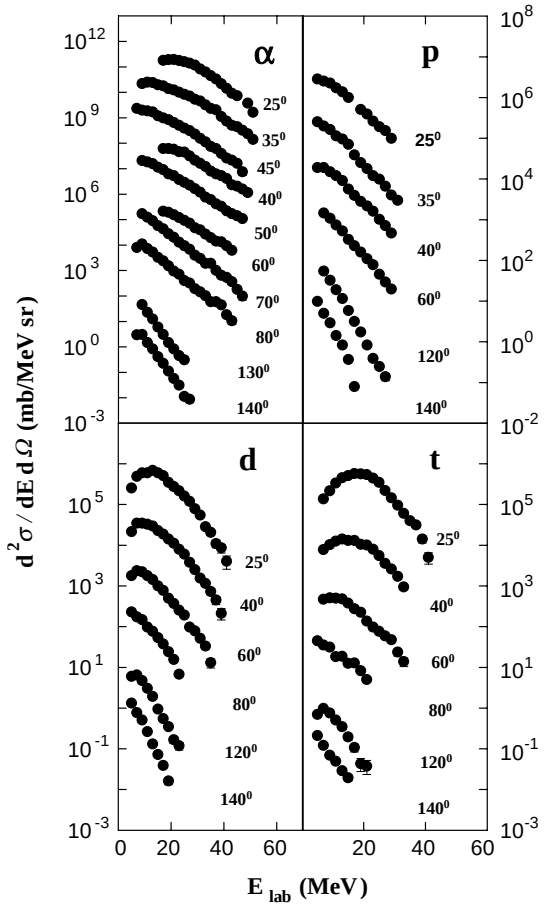

Fig. 1. Inclusive (filled circles) light-charged-particle energy spectra obtained in the ^{7}Li (47 MeV) + ^{24}Mg reaction at different laboratory angles. For each curve, cross-sections at the highest observed angle are multiplied by 10 and the multiplication factor subsequently increases by a factor of 10 for each of the successive curves as the angle decreases.

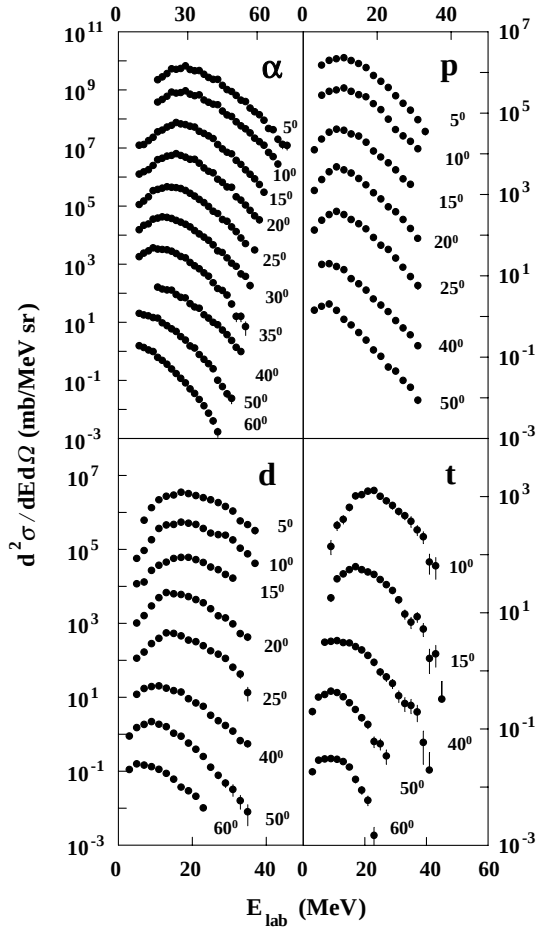

Fig. 2. Same as fig. 1 for the ^{19}F (96 MeV) + ^{12}C reaction.

the reactions ^{64}Ni on ^{100}Mo and ^{16}O on ^{148}Sm. They have shown that the measured spectra deviate from the statistical-model predictions at incident energies above ∼5 MeV/nucleon, and that different set of parameters are required to reproduce the data for different types of light charged particles, such as, α, proton, deuteron and triton. Moreover, the magnitude of the deviation has been found to depend on the excitation energy as well as the entrance channel. Intuitively, the entrance channel dependence may affect the shapes of the light-charged-particle spectra if the equilibrating system remains deformed over a time scale comparable to the mean lifetime of the charged-particle emission. Recent measurements of α-particle energy spectra for the reactions 83, 97 MeV ^{12}C on ^{45}Sc [11] and 110 MeV ^{16}O on ^{54}Fe [10] have also indicated that the role of the entrance channel dynamics should be carefully looked into.

It is thus apparent that there exists some discrepancy between the experimentally measured spectra and the corresponding predictions of the standard statistical model, which is prominent for higher spin and for heavier systems ($A \geq 60$). However, due to the lack of experimental data, the situation is not clear for the lighter systems at relatively lower spin. This prompted us to explore the scenario for light systems, such as, ^{31}P, in the incident energy range below 5 MeV/A. In the present work, we have populated the compound nucleus ^{31}P at excitation energy ∼ 60 MeV through different entrance channels, *i.e.*, 96 MeV ^{19}F on ^{12}C and 47 MeV ^{7}Li on ^{24}Mg and have measured the energy and angular distributions of all light charged particles, (*i.e.*, α, p, d and t). Since the two reaction channels populate the same compound system with different angular-momentum distributions ($l_{\rm cr} \sim 21\hbar$ and $16\hbar$, respectively) it offers an opportunity to study the angular-momentum dependence in the evaporative-decay cascade. Apart from that, entrance channel configurations may also affect the evaporative decay if the nucleus lives in the dinuclear form for a long time and evaporates during this period. But our previous studies on the intermediate-mass fragment emission did not reflect the existence of any such long-lived dinuclear configuration [13,14] of the ^{31}P compound nucleus. Earlier, we have measured also α-particle spectra in coincidence with the evaporation residues in the 96 MeV ^{19}F on ^{12}C reaction [9] and have observed that the measured spectra deviate from the statistical-model predictions both at low

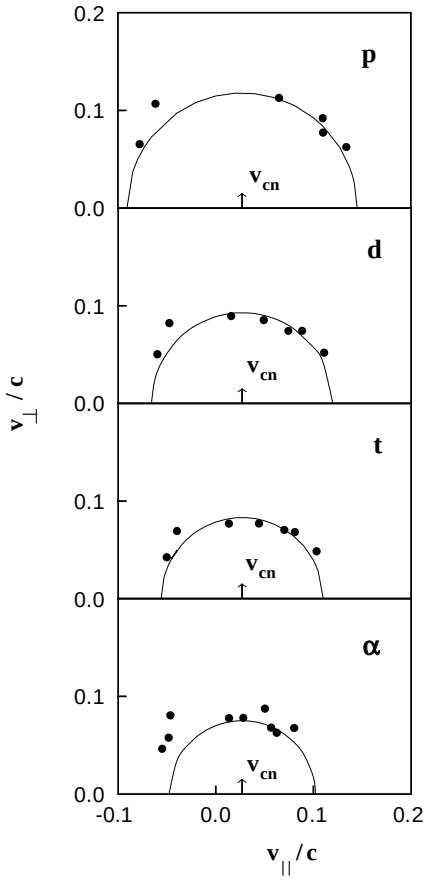

Fig. 3. Average velocities of the light charged particles, obtained in the ^{7}Li (47 MeV) + ^{24}Mg reaction, as a function of velocities parallel ($v_{\parallel}$) and perpendicular ($v_{\perp}$) to the beam direction. The arrows indicate the velocity of the compound nucleus.

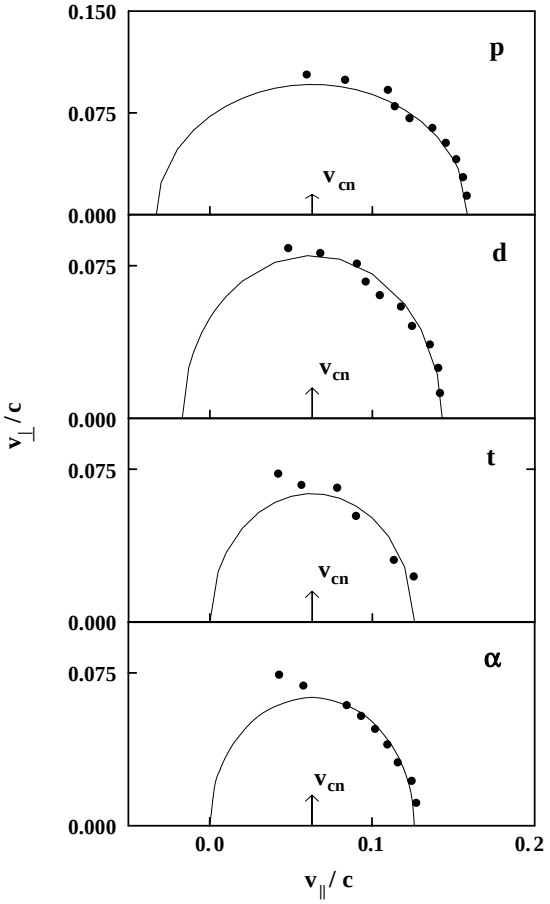

Fig. 4. Same as fig. 3 for the ^{19}F (96 MeV) + ^{12}C reaction.

as well as at high-energy sides. Assuming a deformed configuration of the compound nucleus, the full energy spectra could be explained satisfactorily. Interestingly, it has been observed in earlier works that, different amount of deformations are required to explain different sets of light-charged-particle data. It directly points to the inadequacy of the standard statistical model to explain the behaviour of light-charged-particle emission spectra with increasing spin and excitation energy. In the present work, we would like to explore systematically the scenario of light-charged-particle emission further for a lighter system at moderate spin and excitation energy.

The paper has been arranged as follows. The experimental details along with the experimental results are described in sect. 2. The predictions of the statistical model for the ^{31}P nucleus have been discussed in sect. 3. Finally, the summary and conclusions are presented in sect. 4.

2 Experiments and results

The experiments were performed at the Bhabha Atomic Research Centre - Tata Institute of Fundamental Research 14 UD pelletron accelerator laboratory, Mumbai, with 96 MeV ^{19}F beam on 125 μg/cm^2 self-supporting ^{12}C target and 47 MeV ^{7}Li beam on 275 μg/cm^2 self-supporting $^{\rm nat}$Mg target. The beam current was typically 20–80 nA. The light charged particles have been detected in three solid-state telescopes. The telescopes (T_1, T_2, T_3) were of two elements, consisting of 100 μm, 45 μm, 40 μm ΔE Si(SB) and 5 mm, 5 mm, 2 mm Si(Li) E detectors, respectively. Typical solid angles were 1.5 msr, the same for all the three telescopes. Analog signals from the detectors were processed using the standard electronics before being fed to the computer for on-line data acquisition.

The telescopes were calibrated with the radioactive ^{228}Th α-source. Typical energy resolutions (FWHM) obtained were 1.12% for T_1 and 1.13% for T_2 and T_3, respectively. The low-energy cutoffs thus obtained were typically 3 MeV for proton, 5 MeV for deuteron, 5 MeV for triton and 11 MeV for α in T_1. In T_2 and T_3 cutoffs were 1 MeV for proton, 3 MeV for deuteron, 3 MeV for triton and 7 MeV for α-particles.

Inclusive energy distributions for α-particles, proton, deuteron and triton have been measured in an angular range of 25°–140° in the case of ^{7}Li (47 MeV) + $^{\rm nat}$Mg reaction and in a range of 5°–60° in the case of ^{19}F (96 MeV) + ^{12}C reaction. In the centre-of-mass (c.m.) frame it covers up to $\sim$ 140° in both cases. Figures 1-2 show the

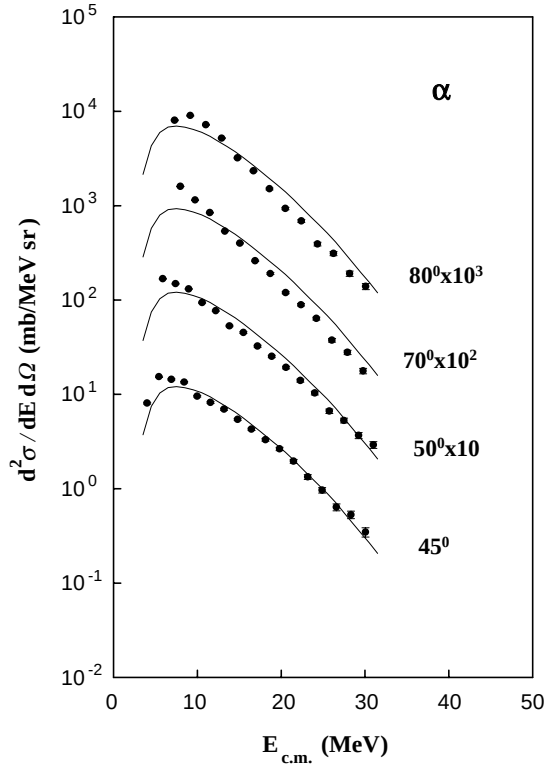

Fig. 5. Inclusive (filled circles) α-particle energy spectra, obtained in the ^{7}Li (47 MeV) + ^{24}Mg reaction, in the centre-of-mass frame measured at different laboratory angles. Solid lines (normalized at the peak of the measured data) are the predictions of CASCADE calculations with the standard value of the radius parameter, r_0 (see text).

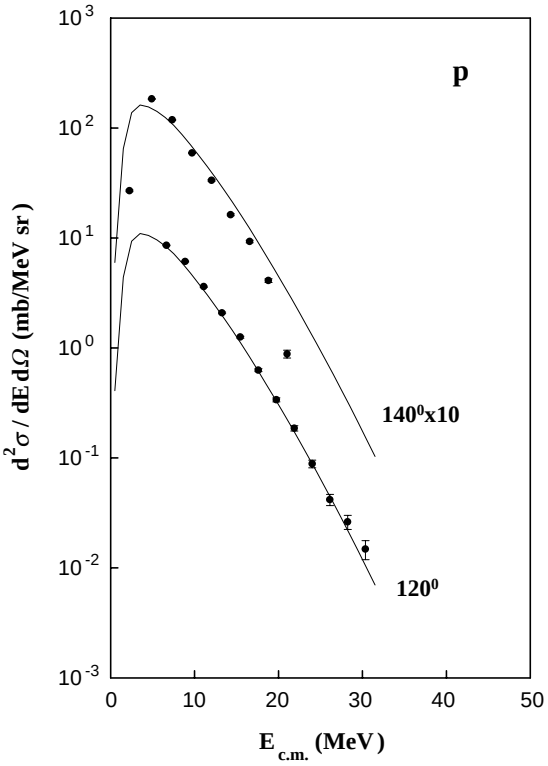

Fig. 6. Same as fig. 5 for protons.

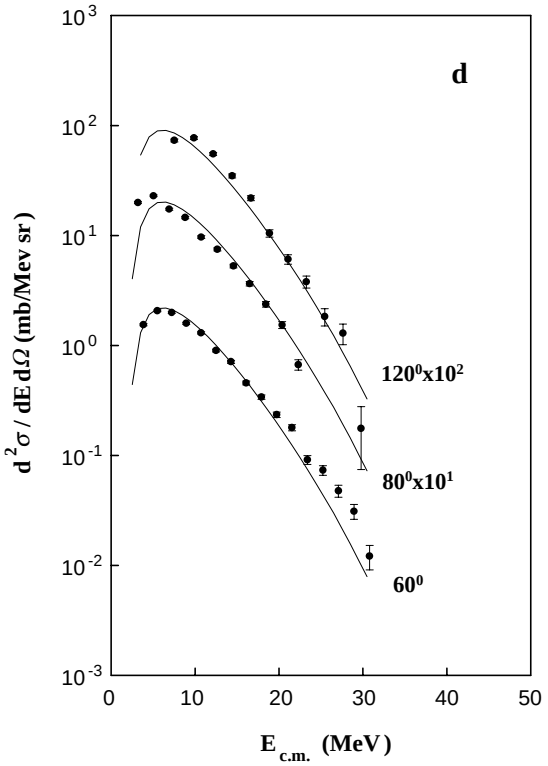

Fig. 7. Same as fig. 5 for deuterons.

measured-energy spectra for the light charged particles at different laboratory angles respectively for the two reactions. The shape of the energy spectra is similar for all the measured angles indicating the fact that the thermal equilibrium has been achieved in both the cases before the particle emission.

The average velocities of the observed light charged particles have been plotted in the parallel ($v_\parallel$) and perpendicular ($v_\perp$) velocity plane (figs. 3-4) for the ^{7}Li (47 MeV) + ^{24}Mg and ^{19}F (96 MeV) + ^{12}C reactions. It has been observed, that for all particles, the average velocities fall on a circle around the compound-nucleus velocities ($v_{\rm cn}$). It implies that the average velocities (as well as the average kinetic energies) of the light charged particles are independent of the centre-of-mass emission angles in both the reactions. It means that the energy relaxation is complete and the light charged particles are emitted from a fully equilibrated source moving with the velocity $v_{\rm cn}$. The deviations in average velocity of the light charged particles at backward angles ($\theta_{\rm lab} \geq 40^\circ$) are due to large energy cutoffs in the energy spectra.

3 Discussion

The experimental data have been compared with the predictions of standard statistical-model calculation using

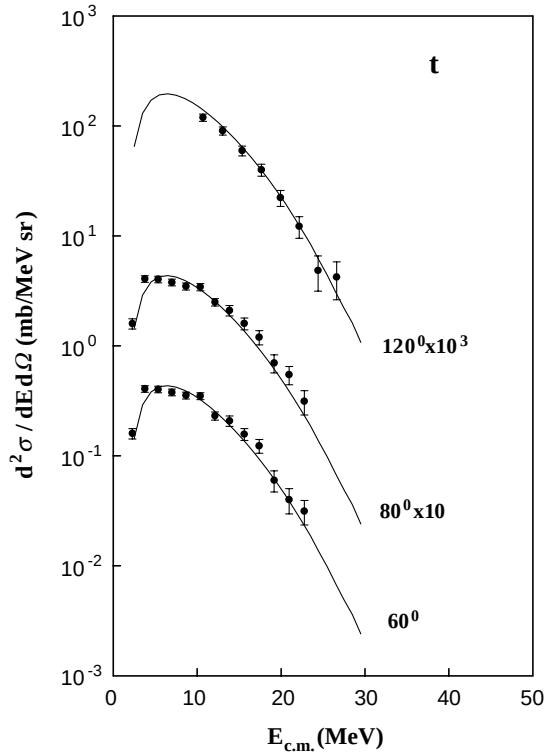

Fig. 8. Same as fig. 5 for tritons.

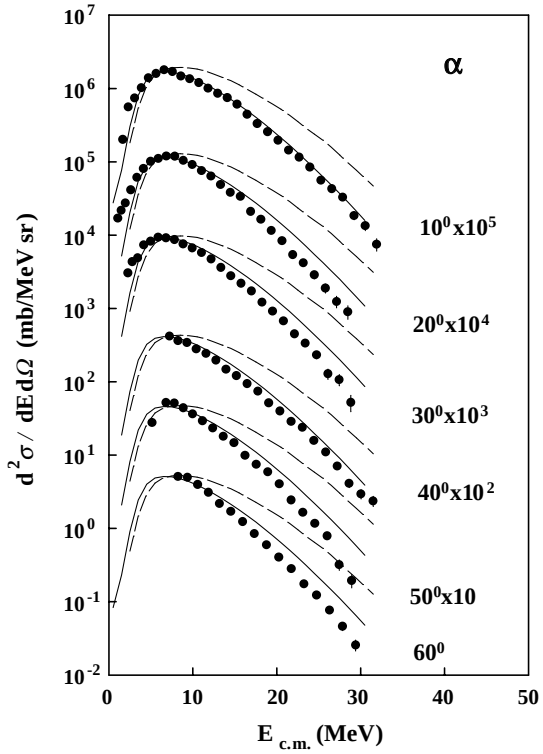

Fig. 9. Inclusive (filled circles) α-particle energy spectra, obtained in the ^{19}F (96 MeV) + ^{12}C reaction, in the centre-of-mass frame measured at different laboratory angles. Curves are the predictions of CASCADE calculations with the standard (dashed curves) and the modified (solid curves) values of the radius parameter, r_0 (see text). Curves are normalized at the peak of the measured data.

the code CASCADE [15]. Figures 5-8 show the centre-of-mass energy spectra for the various light charged particles, such as α, p, d and t, observed in the ^{7}Li (47 MeV) + ^{24}Mg reaction. The solid lines represent the predictions of the statistical-model code CASCADE. The optical-model parameters used for calculating the transmission coefficients were taken from [16] for p, d, t, and from [17] for α-particles. The critical angular momentum for fusion, $l_{\rm cr}$, is calculated using the Bass model as $16\hbar$ [18]. Sharp cutoff angular-momentum distribution has been assumed. The radius parameter was taken to be 1.29 fm following Pühlhofer *et al.* [15]. The angular-momentum–dependent deformation parameters (δ_1 and δ_2 as described later) were set equal to zero. From the figures, it is observed that the theoretical predictions match well with the experimental results, indicating that all the light charged particles are evaporated from a nearly spherical ^{31}P compound nucleus.

However, in the case of ^{19}F (96 MeV) + ^{12}C reaction, the statistical-model calculation using the code CASCADE, with the standard parameter set, fails (dashed lines) to predict the shape of the experimental spectra. Figures 9-12 show the observed (filled circles) and calculated (solid and dashed lines) centre-of-mass energy spectra for the various light charged particles emitted in the ^{19}F (96 MeV) + ^{12}C reaction. The figures indicate a deviation of the experimental data from the standard statistical-model predictions (dashed lines) at low- as well as at high-energy sides of the spectra.

According to the CASCADE calculations, the lower-energy part of the spectra is controlled by the transmission coefficients. For the calculation of transmission coefficients, we have used the same sets of optical-model parameters as in the case of ^{7}Li (47 MeV) + ^{24}Mg reaction, (*i.e.*, the optical-model parameters from [17] for alpha particles, and from [16] for proton, deuteron and triton). A deformed configuration of the compound nucleus has been assumed in the calculation. This is realized by varying only the radius parameter r_0. The optimum value of r_0 is found to be ~ 1.56 fm which is consistent with our earlier work [9]. The increased radius parameter lowers the emission barrier and hence enhances the low-energy yield by increasing the transmission coefficients.

The higher-energy part of the spectra is controlled by the level density $\rho(E, j)$, which for a given angular momentum j and excitation energy E is defined as [15]

$$\rho(E,j) = \frac{2j+1}{12} a^{1/2} \left(\frac{\hbar^2}{2\mathcal{J}_{\rm eff}}\right)^{3/2} \frac{1}{(E+T-\Delta-E_j)^2} \times \exp[2[a(E-\Delta-E_j)]^{1/2}], \quad (1)$$

where a is the level density parameter, which is taken to be $A/8$ for the present calculation, T is the thermodynamic temperature, Δ is the pairing correction, and E_j is the rotational energy which can be written in terms of the

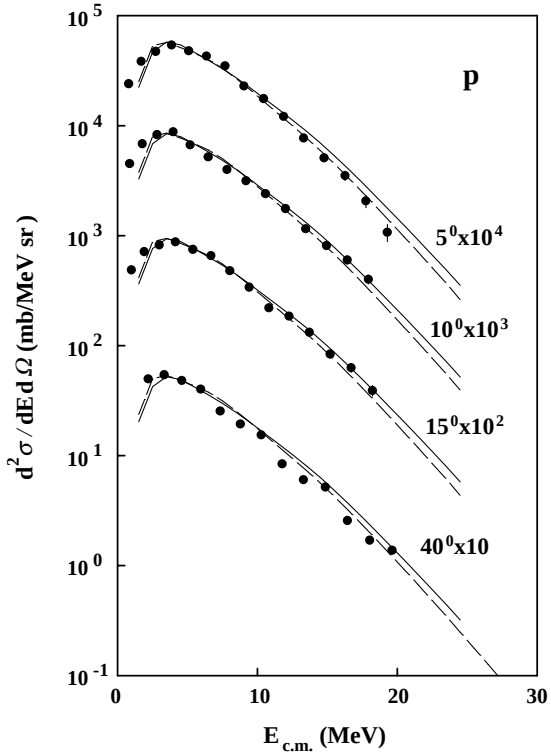

Fig. 10. Same as fig. 9 for protons.

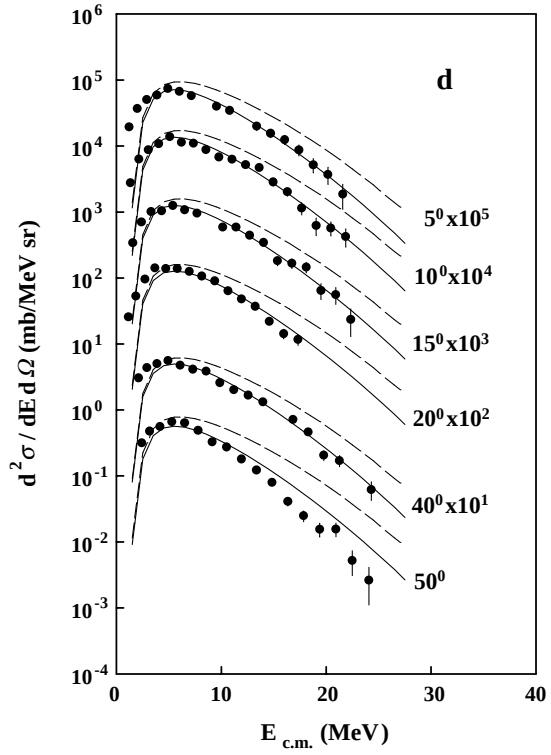

Fig. 11. Same as fig. 9 for deuterons.

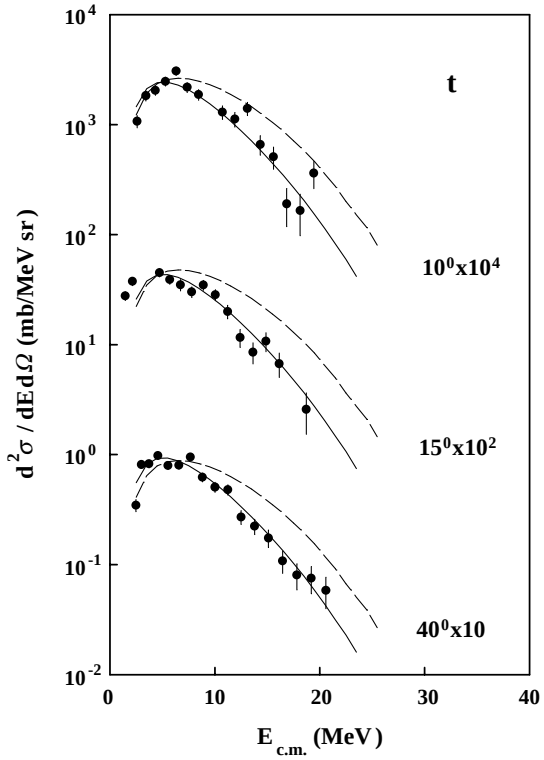

Fig. 12. Same as fig. 9 for tritons.

effective moment of inertia $\mathcal{J}_{\rm eff}$ as

$$E_j = \frac{\hbar^2}{2\mathcal{J}_{\rm eff}} j(j+1). \tag{2a}$$

In hot rotating nuclei, formed in heavy-ion reactions, the effective moment of inertia may be spin dependent and may be written as

$$\mathcal{J}_{\rm eff} = \mathcal{J}_0 \times (1 + \delta_1 j^2 + \delta_2 j^4), \tag{2b}$$

where, the rigid-body moment of inertia, $\mathcal{J}_0$, is given by

$$\mathcal{J}_0 = \frac{2}{5} A^{5/3} r_0^2. \tag{2c}$$

Here, A is the mass number and r_0 is the radius parameter. Non zero values of the parameters δ_1, δ_2 introduce the spin dependence in the effective moment of inertia (eq. (2b)). The relation (eq. (2a)) defines a region in the energy, angular-momentum plane ($(E$-$j)$-plane) of allowed levels and a region where no levels occur. The region is bounded by the yrast line defined by the lowest-energy state that occurs for a given angular momentum. It has been observed in the previous experiments [5,9] that the yrast line has to be modified to explain the experimental data. Different attempts have been pursued using different tools to modify the yrast line, such as, radius parameter r_0, deformation parameters δ_1, δ_2 and the angular momentum j.

However, we have observed that the variation of a single input parameter, r_0, in the code CASCADE, is suffi-

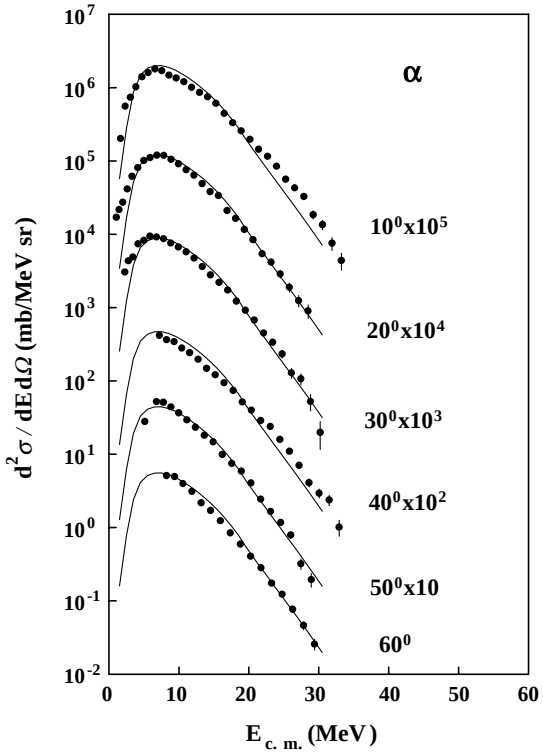

Fig. 13. Inclusive c.m. α-particle energy spectra at different laboratory angles, obtained in the ^{19}F (96 MeV) + ^{12}C reaction. Solid lines (normalized at the peak of the measured data) are the predictions of CASCADE with $\delta_1 = 2.8 \times 10^{-3}$ and $\delta_2 = 2.5 \times 10^{-7}$ (see text).

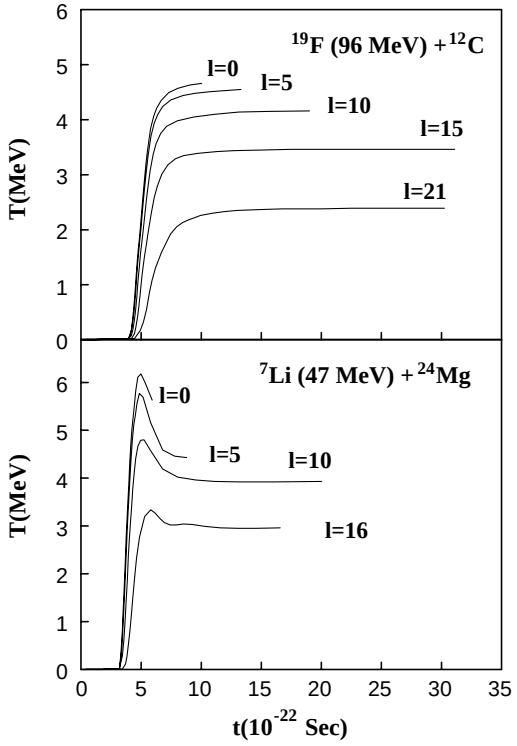

Fig. 14. Time evolution of the temperature (T) parameter as obtained from HICOL calculations for the reactions studied.

cient to take care of the low energy as well as the high-energy side of the spectra [9]. So, in the present calculation, we varied the parameter r_0 only, and kept the spin-dependent parameters δ_1, δ_2 in eq. (2b) equal to zero, to reproduce the experimental spectra. It is clear from figs. 9-12 that the calculated spectra (solid lines) agree quite well with the experimental spectra both in the low-energy as well as in the high-energy regions.

For the sake of completeness, we also attempted to interpret the data using the other alternative; *i.e.*, by introducing angular-momentum dependence in the effective moment of inertia through the angular-momentum–dependent deformation parameters, *i.e.*, δ_1, δ_2 of eq. (2b). The best-fit values δ_1 and δ_2 obtained from fitting the data were $\delta_1 = 2.8 \times 10^{-3}$ and $\delta_2 = 2.5 \times 10^{-7}$. Representative theoretical predictions with the above best-fit parameters have been shown in fig. 13 along with the respective experimental data for the α-particles emitted in ^{19}F (96 MeV) + ^{12}C reaction. It is clearly seen that with the above values of δ_1 and δ_2, the predicted spectra match well with the experimental ones. It is further evident (comparing fig. 13 with fig. 9) that both the prescriptions (either changing r_0 only or varying δ_1 and δ_2) yield nearly equivalent result, at least for the system considered here.

In order to probe more deeply into the matter, we have estimated an average radius parameter (for non zero values of δ_1 and δ_2) by averaging over the angular-momentum distribution (sharp cutoff triangular distribution has been assumed, up to the critical angular momentum $21\hbar$) in the following way:

$$r_{\rm eff}^2 = r_0^2 \frac{\sum_0^{j_{\rm cr}} (1 + \delta_1 j^2 + \delta_2 j^4)(2j+1)}{\sum_0^{j_{\rm cr}} (2j+1)} \qquad (3)$$

Here, r_0 is taken as 1.29 fm. $j_{\rm cr}$ is the critical angular momentum of the system. δ_1 and δ_2 values are as stated above. The effective radius parameter, $r_{\rm eff}$, thus obtained is 1.65 fm which is within 10% of the radius parameter we have used in the statistical-model calculation to reproduce the experimental data. Therefore, it can be said that the variation of the single parameter r_0 to fit the data is nearly equivalent to the spin-dependent level density prescription as described above, at least for light compound systems involving lower spins.

For such light compound systems like ^{31}P at low spins, the present method has a distinct advantage. Here, both lower- and higher-energy side of the spectra could be fitted by changing a single parameter r_0, once for all. The increase of r_0 causes lowering of the barrier which enhances the transmission coefficient, thereby correcting the lower-energy side of the spectra; at the same time, it also causes a reduction of the rotational energy thereby changing the level density in the right direction to explain the high-energy part of the spectra. On the contrary, in the standard spin-dependent level density prescription, one has to take care of the low-energy side of the spectra separately by introducing a reduced barrier. However it may be noted that, as the spin-dependent deformation becomes

more significant at higher spins, the present method may not lead to realistic values of r_0 for higher spins; in such cases one may have to consider the spin-dependent deformation only. On the other hand, for lower-spin values, (for example, the compound nucleus ^{31}P formed in the reaction ^{7}Li (47 MeV) + ^{24}Mg with $l_{\rm cr} \sim 16\hbar$) the change in r_0 may not be quite appreciable. This intuitively explains why the standard statistical-model predictions have been in good agreement with the data in this case.

We have also tried to estimate the effect of entrance channel dynamics on light-charged-particle emission using the code HICOL [19]. Figure 14 shows the calculated temperature of the fused nuclei as a function of time for various angular-momentum values covering the range of interest for the two reactions under study. From fig. 14, it is observed that for both cases, thermal equlibration of the system is achieved, on the average, within 8×10^{-22} s after the zero time. The zero time is defined as the time when the participating nuclei begin to feel the nuclear forces and deviate from their earlier Coulomb trajectories. It is also observed that the temperature decreases with increasing angular momentum. Decay time has been estimated to be $\sim 12 \times 10^{-22}$ s, using the code PACE2, which is comparable to the formation time of the nucleus as obtained from HICOL. This implies that the effect of entrance channel on particle emission should be similar in both the reactions. However, particle spectra observed in the two reactions are different, implying that the above difference may not be due to the entrance channel dynamics.

4 Summary and conclusion

We have measured the inclusive light-charged-particle energy spectra in an angular range of 5°–60° and 25°–140°, respectively, in the ^{19}F (96 MeV) + ^{12}C and ^{7}Li (47 MeV) + $^{\rm nat}$Mg reactions. It has been observed from the average velocity plots in the $v_{\parallel}$ *vs.* $v_{\perp}$ plane that the average velocities of all light charged particles in both the reactions stated above fall on the circles centered around their respective compound nuclear velocities, implying that these particles are emitted from equilibrated compound nuclear sources. The data in the two reactions have been compared with the statistical-model calculations using the code CASCADE. It has been observed that the light-charged-particle spectra measured in the ^{7}Li (47 MeV) + ^{24}Mg reaction can be well explained in the framework of standard statistical-model calculation, whereas the light-charged-particle spectra obtained in the ^{19}F (96 MeV) + ^{12}C reaction deviate significantly from similar calculations. The formation times as estimated by the semiclassical calculation using the code HICOL and the decay times as estimated by PACE2 are comparable in both cases. Therefore, the discrepancy in the light-charged-particle spectra obtained in the two reactions may not be due to the entrance channel effect as the estimated formation and decay times of the compound nucleus in both cases are of the same order. Rather, it may be attributed to the difference in the angular-momentum distributions of the compound nuclei formed in the two reactions considered here. A satisfactory description of the measured-energy spectra in the case of ^{19}F (96 MeV) + ^{12}C has been achieved by invoking a deformed configuration of the compound nucleus through the modification of the radius parameter r_0 from 1.29 fm to 1.56 fm in the statistical-model calculation. The data could also be reproduced equally well by incorporating spin-dependent level density formalism and the average radius parameter obtained using this prescription is 1.65 fm, which is within 10% of the radius parameter we have used to reproduce the experimental data. However, it may be mentioned here that the present simplified approach may not lead to realistic values of r_0 for larger values of compound-nucleus spin, which may limit the use of this simple approach for heavier compound systems at higher spins. In conclusion, the present work demonstrates that a modified radius parameter (r_0) alone may be sufficient to reproduce the deformations for lighter systems ($A \sim 30$). However, it will be interesting to explore the validity of this simple approach in explaining the light-charged-particle data for heavier systems at higher excitations.

The authors thank the Pelletron operating staff for smooth running of the machine and Mr. D.C. Ephraim of T.I.F.R., for making the targets.

References

1. M.N. Namboodiri, P. Gonthier, H. Ho, J.B. Natowitz, R. Eggers, L. Adler, P. Kasiraj, C. Cerruti, A. Chevarier, N. Chevarier, A. Demeyer, Nucl. Phys. A **367**, 313 (1981).
2. R.K. Choudhury, P.L. Gonthier, K. Hagel, M.N. Namboodiri, J.B. Natowitz, L. Adler, S. Simon, S. Kniffen, G. Berkowitz, Phys. Lett. B **143**, 74 (1984).
3. G. La Rana, D.J. Moses, W.E. Parker, M. Kaplan, D. Logan, R. Lacey, J.M. Alexander, R.J. Welberry , Phys. Rev. C **35**, 373 (1987).
4. I.M. Govil, J.R. Huizenga, W.U. Schröder, J. Toke, Phys. Lett. B **197**, 515 (1987).
5. J.R. Huizenga, A.N. Behkami, I.M. Govil, W.U. Schröder, J. Tõke Phys. Rev. C **40**, 668 (1989).
6. B. Fornal, G. Viesti, G. Nebbia, G. Prete, J.B. Natowitz, Phys. Rev. C **40**, 664 (1989).
7. R.J. Charity, M. Korolija, D.G. Sarantites, L.G. Sobotka, Phys. Rev. C **56**, 873 (1997).
8. I.M. Govil, R. Singh, A. Kumar, J. Kaur, A.K. Sinha, N. Madhavan, D.O. Kataria, P. Sugathan, S.K. Kataria, K. Kumar, Bency John, G.V. Ravi Prasad, Phys. Rev. C **57**, 1269 (1998).
9. D. Bandyopadhyay, S.K. Basu, C. Bhattacharya, S. Bhattacharya, K. Krishan, A. Chatterjee, S. Kailas, A. Navin, A. Srivastava, Phys. Rev. C **59**, 1179 (1999).
10. I.M. Govil, R. Singh, A. Kumar, Ajay Kumar, G. Singh, S.K. Kataria, S.K. Datta, Phys. Rev. C **62**, 064606 (2000).
11. I.M. Govil, R. Singh, A. Kumar, S.K. Datta, S.K. Kataria, Nucl. Phys. A **674**, 377 (2000).
12. R.J. Charity, Phys. Rev. C **61**, 054614 (2000).
13. C. Bhattacharya, D. Bandyopadhyay, S.K. Basu, S. Bhattacharya, K. Krishan, G.S.N. Murthy, A. Chatterjee, S.K. Kailas, P. Singh, Phys. Rev. C **52**, 798 (1995).

14. C. Bhattacharya, D. Bandyopadhyay, S.K. Basu, S. Bhattacharya, K. Krishan, G.S.N. Murthy, A. Chatterjee, S.K. Kailas, P. Singh, Phys. Rev. C **54**, 3099 (1996).
15. F. Pühlhofer, Nucl. Phys. A **280**, 267 (1977).
16. C.M. Perry, F.G. Perry, At. Data Nucl. Data Tables **17**, 1 (1976).
17. J.R. Huizenga, G. Igo, Nucl. Phys. **29**, 462 (1961).
18. R. Bass, *Nuclear Reactions with Heavy Ions* (Springer-Verlag, Berlin, 1980) p. 256.
19. H. Feldmeier, Rep. Prog. Phys. **50**, 915 (1987).